

# Uniplanar UWB-MIMO Antenna with High Isolation Based on a Radiator-Ground Shared Structure

Zhijun Tang\*, Ling Liang, Bin Zhong, Long Cheng, Chao Tan, and Shigang Hu

**Abstract**—This letter presents a uniplanar two-port UWB-MIMO antenna with high isolation for wireless communication applications. The designed antenna is composed of a single metal layer and a thin substrate. The single metal layer acts as radiators and a ground plane. The radiator of each element consists of a modified dual-L-shaped feeding structure and a defected rectangular patch, which is shared by the ground plane. The modified dual-L-shaped feeding structure is introduced to broaden the bandwidth. Furthermore, two fork-shaped slots and bent slots are embedded in the rectangular shared structure for further improving the bandwidth and decreasing the mutual couplings without any other additional decoupling structures. The experimental results show that the proposed antenna achieves the ultra-wide impedance bandwidth (3.0–12.4 GHz), high isolation ( $> 20$  dB at entire impedance bandwidth), very small ECC ( $< 0.01$ ), high multiplexing efficiency ( $> -1.9$  dB), stable realized gain, and radiation patterns. Therefore, the designed antenna is suitable for most wireless UWB communication applications.

## 1. INTRODUCTION

Ultra-Wideband (UWB) is a carrier-free communication technology. It transmits data by using nonsinusoidal narrow pulses at nanosecond to microsecond. In recent years, UWB communication technology has attracted wide attention due to its outstanding advantages such as high transmission rate, large channel capacity, good concealment, precise positioning, strong anti-multipath fading, low hardware cost, and low power consumption [1–4]. Especially since the Federal Communications Commission (FCC) approved the unlicensed allocation of the 3.1–10.6 GHz frequency band to commercial UWB wireless communication systems in 2002, a wave of researches on ultra-wideband communication technology has been triggered. However, FCC has strict restrictions on the radiated power of UWB, which makes the communication distance of UWB wireless communication systems shorter. In order to effectively increase the communication distance of the UWB system, it has been suggested that UWB technology combines the Multiple-Input Multiple-Output (MIMO) technology to form UWB-MIMO technology. Therefore, as a key component of UWB-MIMO systems for transmitting and receiving signals, UWB-MIMO antenna has also gradually attracted attention [5–7].

In general, two most important problems in UWB-MIMO antenna design are how to broaden the bandwidth and improve the isolation. In recent years, many methods or techniques have been adopted for broadening the bandwidth such as many type monopole antennas [8–10], slot antennas [11], gradual structure antennas [12], fractal antennas [13], and meander techniques [14]. On the other hand, the methods or techniques of improving isolation mainly focus on the decoupling structures [15], neutral line [16], orthogonal layout [17], defected ground structure (DGS) [18], electromagnetic band gap (EBG), pattern diversity [19], etc. Most of the existing UWB-MIMO antennas have multiple

---

*Received 28 June 2020, Accepted 4 August 2020, Scheduled 24 August 2020*

\* Corresponding author: Zhi-Jun Tang (zjtang@hnust.edu.cn).

The authors are with the School of Information and Electrical Engineering, Hunan University of Science and Technology, Xiangtan 411201, China.

layer structures, and their radiators and ground plane are independent and separate. However, the compactness of modern wireless terminals or platforms requires the conformal design of antenna structures. Especially, the enclosure or chassis of the terminal acts as not only radiators, but also a ground plane [20]. Recently, this design method of the shared structure is mainly applied in mobile communication terminals, which requires narrow bandwidth and low isolation compared with UWB applications. Therefore, it is important that two key problems of the limited bandwidth and low isolation need to be solved for extending this method to the UWB-MIMO antenna design.

In this letter, a uniplanar two-port UWB-MIMO antenna is designed by using a radiator-ground shared structure. The designed antenna consists of a single rectangular metal layer and a thin substrate. The radiator of each element consists of a modified dual-L-shaped feeding structure and a defected rectangular patch, which is shared by the ground plane. The bandwidth potential of the designed antenna is predicted by using characteristic mode analysis (CMA). The modified dual-L-shaped feeding and loading structure is introduced to excite the desired characteristic modes (CMs) at some relevant resonant frequencies, and thus the structure broadens the bandwidth. Furthermore, the fork-shaped and bent slots are embedded in the rectangular shared structure for partially improving bandwidth and decreasing the mutual couplings without any other additional decoupling structures.

## 2. ANTENNA DESIGN

Physical structure of the proposed antenna is illustrated in Figure 1. Similar to a coplanar waveguide (CPW) fed antenna, the designed antenna also has a uniplanar structure. However, the CPW-fed antenna requires that the ground plane and radiator must be separated and cannot be connected as a whole. Furthermore, its structure design has some specified requirements, and its feed port usually uses an SMA connector. The proposed antenna is a radiator-ground shared structure with a single metal patch. The metal patch acts as radiators and a ground plane.

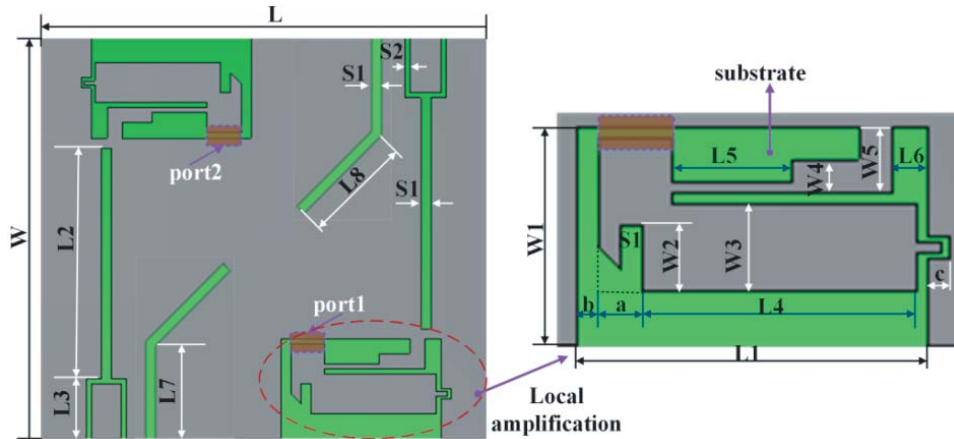


**Figure 1.** Physical structure of the proposed antenna.

The designed antenna consists of a rectangular metal patch and a Rogers3003 substrate ( $\epsilon_r = 3.0$ ,  $\tan \delta = 0.001$ ), and its thickness is 1.6 mm. The designed antenna is printed on the Rogers3003 substrate and fed by two RF coaxial cables. The design procedure of the proposed antenna is described as follows, which is also illustrated in Figure 2.

Firstly, for one element of the antenna, a small rectangular patch is slit from the long side of the metal patch, which makes room for a feeding and loading structure. Based on the quarter-loop structure reported in [19] and the half-loop structure reported in [20], a modified dual-L-shaped loading and feeding structure is designed to excite the desired CMs and broaden the bandwidth. The feeding structure consists of two smaller deformed L-shaped patches. One L-shaped patch is deformed as a stepped patch, and the other is truncated and slit on the corner. The two smaller patches are connected to each other, and one of them is also connected to the shared rectangular patch. Two elements of the

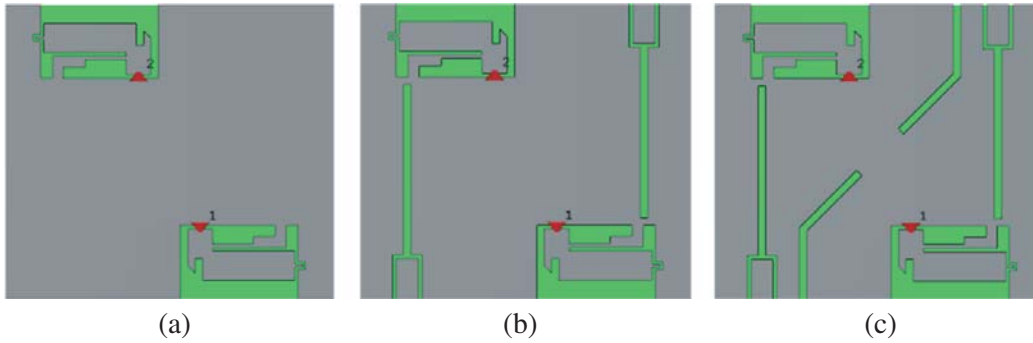


**Figure 2.** Design procedure of the proposed antenna. (a) Antenna #1, (b) Antenna #2, (c) Antenna #3.

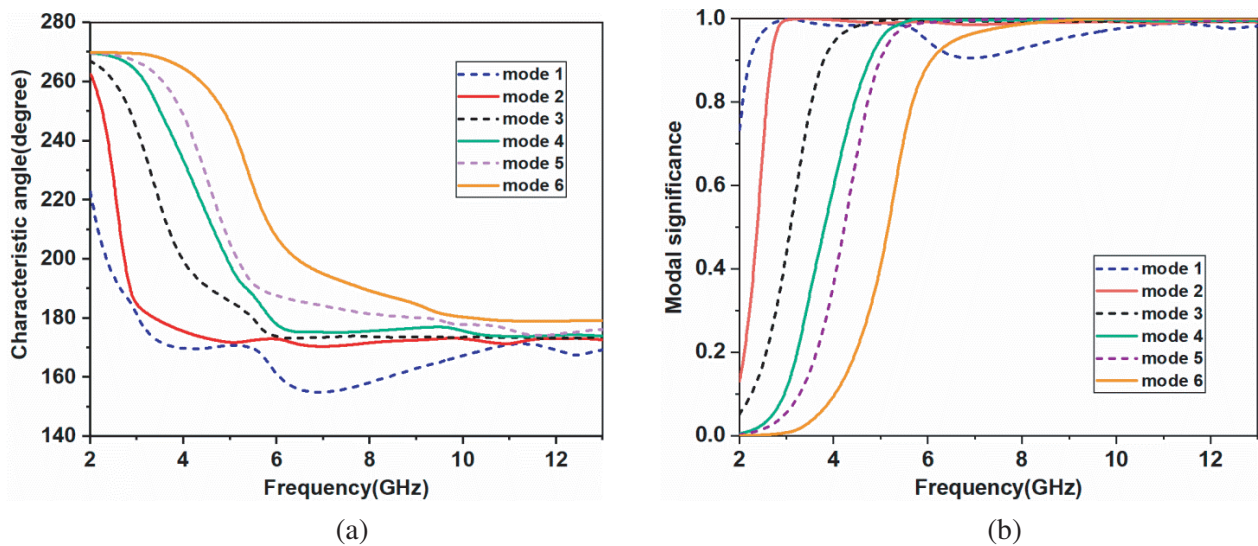


**Figure 3.** Predicted the six most relevant CMs at the UWB band. (a) Characteristic angles, (b) Modal significances.

antenna are identical, and they are located on the opposite edges. This design process of the antenna is called Antenna #1.

Then, we investigate the bandwidth potential of Antenna #1 based on its characteristic mode analysis (CMA). As shown in Figure 3(a), the first six most relevant CMs of the antenna resonate at 3.0 GHz, 3.4 GHz, 5.5 GHz, 6.0 GHz, 9.2 GHz, and 10.2 GHz, respectively. Furthermore, the characteristic angles (CAs) of mode 1 and mode 2 are near 180 degrees at the entire UWB. It is shown that the two modes have ultra-wide bandwidth potential. The CAs of the other CMs are all near 180 degrees from its own resonant frequency to the higher frequency. It also shows that the other CMs have broader bandwidth potentials. The corresponding predicted modal significances (MSs) of the six CMs are shown in Figure 3(b), which further confirms the ultra-wide bandwidth potential of the designed antenna.

Secondly, in order to improve the impedance bandwidth and isolation, two longer fork-shaped slots are etched on the metal layer of Antenna #1. This design process of the antenna is called Antenna #2.

Finally, two bent slots are etched on Antenna #2 for further decreasing the mutual couplings between the two elements at the lower frequency band (below 4.0 GHz). This design process of the antenna is called Antenna #3.

To verify the design effectiveness of the proposed antenna, the *S*-parameters analysis is carried out by CST STUDIO SUITE. The reflection coefficients ( $S_{11}$  or  $S_{22}$ ) of the three antennas are shown

in Figure 4(a). It is observed that the impedance matching is not good for the frequency ranges of 3.8–4.6 GHz, 6.7–7.5 GHz, and 8.2–9.3 GHz in Antenna #1. However, it has improved with a further modification from Antenna #1 to Antenna #2 and Antenna #3.

On the other hand, by etching fork-shaped slots, the isolations ( $S_{12}$  or  $S_{21}$ ) of the antenna are improved at higher frequency band (7.5–11.0 GHz), and the isolations of the antenna at lower frequency band (< 5.2 GHz) are improved evidently by etching the bent slots, which are shown in Figure 4(b). Therefore, the  $S$ -parameters indicate that the proposed antenna has ultra-wide bandwidth and higher isolation.

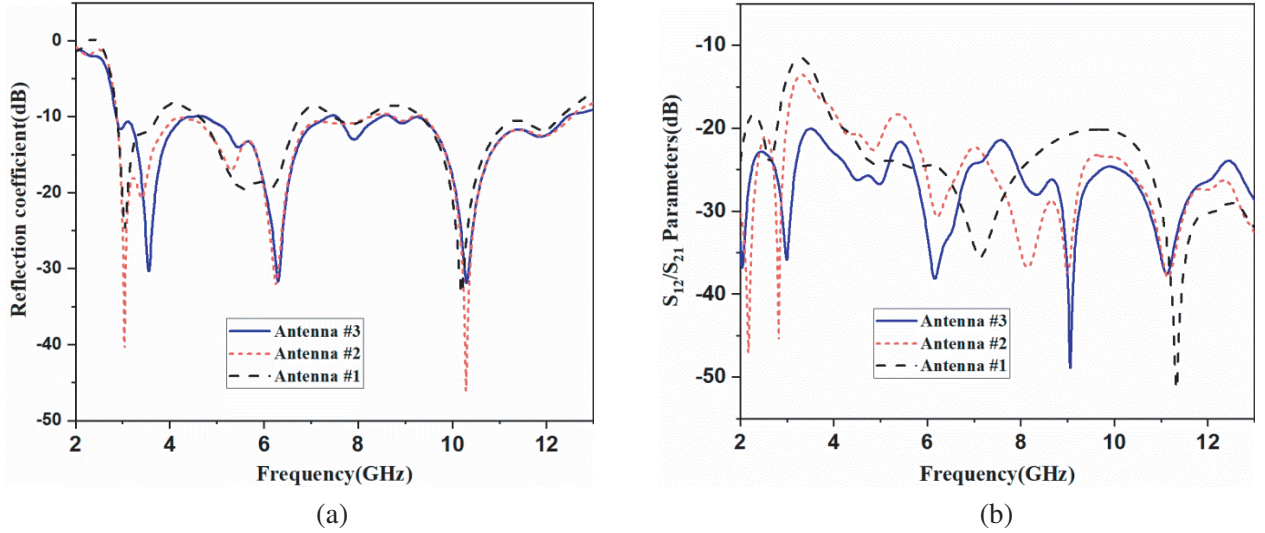


**Figure 4.**  $S$ -parameters of three designed antenna. (a)  $S_{11}$  or  $S_{22}$ , (b)  $S_{12}$  or  $S_{21}$ .

### 3. RESULTS AND DISCUSSION

The optimized geometry parameters of the proposed antenna are shown in Table 1. The reflection coefficient ( $S_{11}$  or  $S_{22}$ ) of the antenna is described in Figure 5(a), which shows that the measured values are consistent with the simulated ones. The antenna has an ultra-wide bandwidth of 9.4 GHz (3.0–12.4 GHz) and a fractional bandwidth of 124.2%. Therefore, the impedance bandwidth of the antenna completely covers the UWB. Furthermore, the antenna resonates at multiple frequencies, which is corresponding to the results of characteristic mode analysis.

**Table 1.** The optimized geometry parameters of the proposed antenna.

Parameter	$L$	$L1$	$L2$	$L3$	$L4$	$L5$	$L6$	$W$	$W1$	$L7$
Value (mm)	45	16.8	23	6	12.6	5.5	1.0	40	10	9.8
Parameter	$W2$	$W3$	$W4$	$W5$	$a$	$b$	$c$	$S1$	$S2$	$L8$
Value (mm)	3.0	4.0	1.5	3.0	2.0	1.6	1.5	1	0.5	11

The isolation performance ( $S_{12}$  or  $S_{21}$ ) of the designed antenna is illustrated in Figure 5(b). It can be observed that the isolation is larger than 20 dB at the frequency range from 2.0 GHz to 13.0 GHz. Furthermore, the isolation is larger than 22 dB at most frequencies of the impedance bandwidth, and the maximal isolation is larger than 48.0 dB. Therefore, the antenna achieves higher isolation or lower mutual coupling at entire impedance bandwidth (3.0–12.4 GHz).

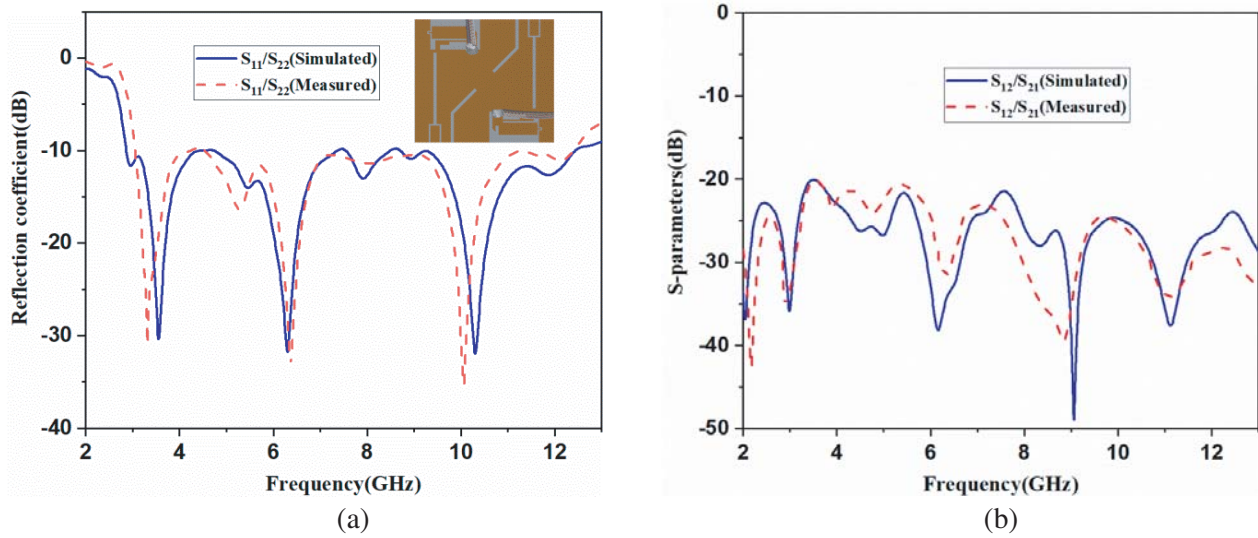


Figure 5. The  $S$ -parameters of the proposed antenna. (a)  $S_{11}$  or  $S_{22}$ , (b)  $S_{12}$  or  $S_{21}$ .

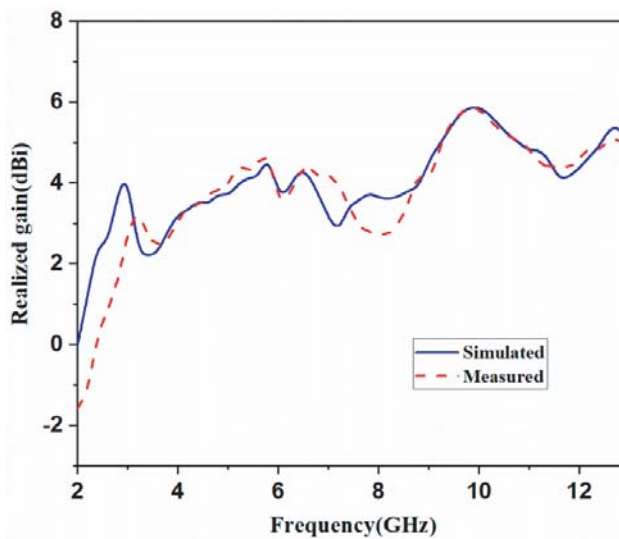
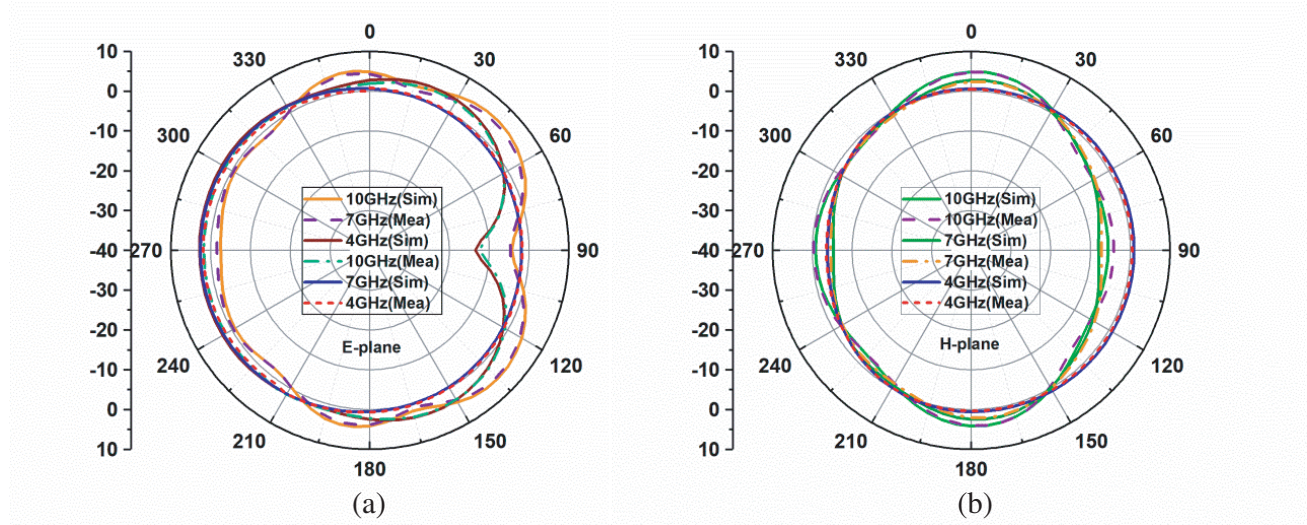


Figure 6. The realized gain of the proposed antenna.

The simulated and measured results of the maximal realized gain are shown in Figure 6. It can be observed that the proposed antenna has relatively stable gain. Furthermore, it varies from 2.4 dBi to 5.8 dBi at the entire impedance bandwidth (3.0–12.4 GHz). Considering the ultra-wide bandwidth, the variation of the realized gain is acceptable for most engineering applications. Figure 7 shows the radiation patterns of the designed antenna at sample frequencies of 4.0 GHz, 7.0 GHz, and 10.0 GHz. It shows that the antenna achieves a stable radiation performance.

The diversity gain and multiplexing efficiency of the proposed antenna are illustrated in Figure 8(a). The diversity gain is near 10.0 dB at the entire impedance bandwidth, and it decreases from 9.95 dB to 8.2 dB at the lower frequency range (below 3.0 GHz). The multiplexing efficiency varies from  $-1.9$  dB to  $-0.1$  dB at the entire impedance bandwidth, and it also decreases from  $-0.2$  dB to  $-7.8$  dB at the lower frequency range (below 3.0 GHz). Therefore, the designed antenna achieves high diversity gain and multiplexing efficiency at the entire impedance bandwidth.

The envelope correlation coefficient (ECC) of the designed antenna is described in Figure 8(b). It



**Figure 7.** The radiation patterns of the proposed antenna. (a) *E*-plane, (b) *H*-plane.

is observed that the ECC value is less than 0.01 at the entire impedance bandwidth, and it increases at the lower frequency range (below 2.8 GHz). Therefore, the antenna has very small ECC values.

Table 2 shows a comparison of some representative UWB-MIMO antennas and radiator-ground shared structure antennas published in recent years. Although the comparison is not comprehensive, it almost represents the current state-of-the-art of UWB-MIMO technology and radiator-ground shared structure technology. Although the size of the proposed antenna is slightly larger than that of some existing UWB-MIMO antennas with a monopole and DGS structure, the design method of the radiator-ground shared structure is successfully extended to the UWB-MIMO antenna design. Furthermore, compared with some existing UWB-MIMO antennas, the characteristics of the proposed antenna are mainly reflected in the number of metal layers and conformal design. Therefore, the proposed antenna achieves a good trade-off of the compactness, bandwidth, gain, radiation pattern, isolation, and ECC.

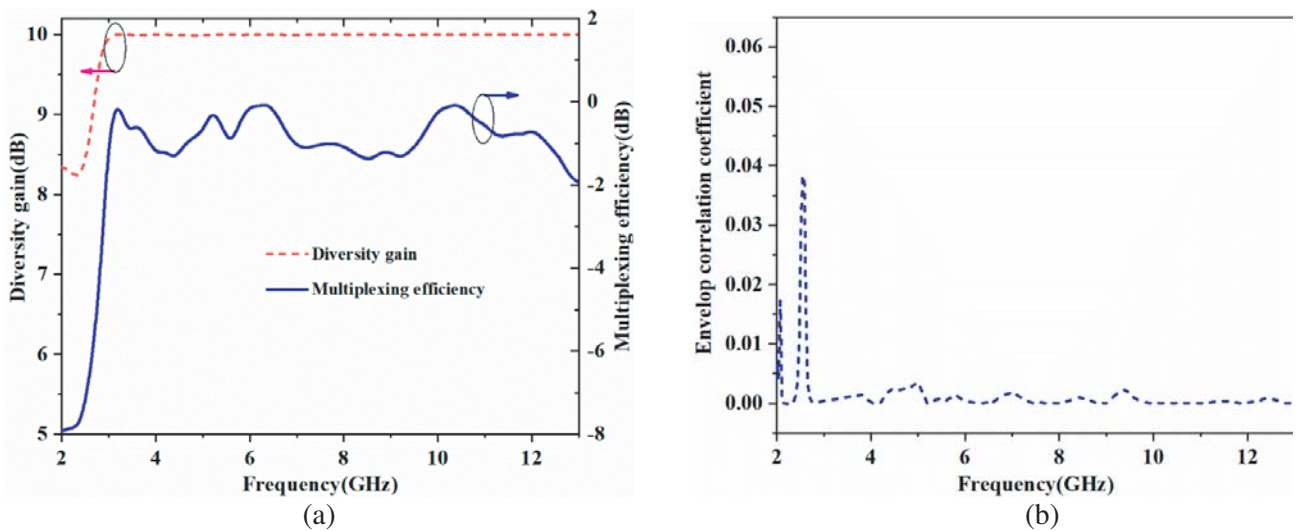


**Figure 8.** The diversity characteristics of the proposed antenna. (a) The diversity gain and multiplexing efficiency, (b) The ECC performance.

**Table 2.** Performance comparison of several typical published literatures.

References	Size (mm <sup>2</sup> )	Bandwidth (GHz)	Gain (dBi)	Isolation (dB)	ECC	Structure
Ref. [5]	23 × 40	2–11	2.0–6.0	> 17	< 0.15	Monopole and DGS
Ref. [7]	50 × 40	2.7–12.0	2.0–5.7	> 17	< 0.03	Monopole and DGS
Ref. [12]	34 × 18	2.93–20.0	0–7.0	> 22	< 0.01	Monopole and DGS
Ref. [13]	24 × 30	3–12.6	2–4.8	> 16.3	< 0.05	Fractal Monopole and DGS
Ref. [15]	40 × 40	3.1–11	1.3–4.0	> 20	< 0.01	Monopole and DGS
Ref. [17]	35 × 35	3.0–12.0	3.0 stable	> 15	< 0.07	Monopole and DGS
Ref. [18]	19 × 30	3.1–10.6	1.2–2.91	> 18	< 0.03	Monopole and DGS
Ref. [19]	50 × 85	2–9.5	1.5–4.0	> 20	< 0.03	Partially shared
Ref. [20]	40 × 100	GSM-LTE bands	NA	> 20	NA	Radiator-ground shared
This work	40 × 50	3.0–12.4	2.4–5.8	> 20	< 0.01	Radiator-ground shared

#### 4. CONCLUSION

In this letter, we have designed and investigated a uniplanar UWB-MIMO antenna based on a shared structure. The shared structure of the radiator and ground plane is introduced to meet the compact and conformal design requirements of current wireless UWB communication applications. The modified dual-L-shaped patches are etched on the shared structure for broadening the bandwidth. In order to further partially improve the bandwidth and decrease the mutual couplings between two elements, two fork-shaped and bent slots are also etched on the shared structure. The simulated and measured results show that the designed antenna achieves a good trade-off, and it can satisfy the communication requirements of the most UWB systems.

#### ACKNOWLEDGMENT

This work was supported by the National Natural Science Foundation of China (Grant Nos. 61875054, 61905074, 61674056); Hunan Provincial Natural Science Foundation of China (Grant Nos. 2020JJ4318, 2019JJ50170); Science research project of Hunan University of Science and Technology (Grant No. KJ1812).

#### REFERENCES

1. Bharadwaj, R. and S. K. Koul, "Experimental analysis of ultra-wideband body-to-body communication channel characterization in an indoor environment," *IEEE Trans. Antennas Propag.*, Vol. 67, No. 3, 1779–1789, 2019.
2. Li, M. J. and N. Behdad, "A compact, capacitively fed UWB antenna with monopole-like radiation characteristics," *IEEE Trans. Antennas Propag.* Vol. 65, No. 3, 1026–1035, 2017.
3. Tang, Z. J., X. F. Wu, and J. Zhan, "A novel miniaturized antenna with multiple band-notched characteristics for UWB communication applications," *Journal of Electro. Waves and App.*, Vol. 32, No. 5, 1961–1972, 2018.
4. Li, Y. S., W. X. Li, and R. Mittra, "Miniaturized CPW-fed UWB antenna with dual frequency rejection bands using stepped impedance stub and arc-shaped parasitic element," *Microw. Opt. Technol. Lett.*, Vol. 56, 783–787, 2014.
5. Thakur, E., N. Jaglan, S. D. Gupta, and B. K. Kanaujia, "A compact notched UWB MIMO antenna with enhanced performance," *Progress In Electromagnetics Research C*, Vol. 91, 39–53, 2019.

6. Liu, Y. Y. and Z. H. Tu, "Compact differential band-notched stepped-slot UWB-MIMO antenna with common-mode suppression," *IEEE Antennas Wireless Propag. Lett.*, Vol. 16, 593–595, 2017.
7. Khan, S. M., A. Iftikhar, S.M. Asif, A. D. Capobianco, and B. D. Braaten, "A compact four elements UWB MIMO antenna with on-demand WLAN rejection," *Microwave and Opt. Techn. Lett.*, Vol. 58, No. 2, 270–276, 2016.
8. Rajkumar, S., A. Amala Anto, and K. T. Selvan, "Isolation improvement of UWB MIMO antenna utilising molecule fractal structure," *Electron. Lett.*, Vol. 55, No. 10, 576–579, 2019.
9. Dastranj, A., "A compact dual-element uniplanar antenna for portable broadband MIMO systems," *Progress In Electro. Research Lett.*, Vol. 73, 113–120, 2018.
10. Yang, Z. X., H. C. Yang, J. S. Hong, and Y. Li, "A miniature triple band-notched MIMO antenna for UWB application," *Microwave Opt. Technol. Lett.*, Vol. 58, No. 3, 642–647, 2016.
11. Luo, C. M., J. S. Hong, and L. L. Zhong, "Isolation enhancement of a very compact UWB-MIMO slot antenna with two defected ground structures," *IEEE Antennas Wireless Propag. Lett.*, Vol. 14, 1766–1769, 2015.
12. Chandel, R., A. K. Gautam, and K. Rambabu, "Tapered fed compact UWB MIMO-diversity antenna with dual band-notched characteristics," *IEEE Trans. Antennas Propag.*, Vol. 66, No. 4, 1677–1684, 2018.
13. Gurjar R., D. K. Upadhyay, B. K. Kanaujia, and A. Kumar, "A compact modified Sierpinski carpet fractal UWB MIMO antenna with square-shaped funnel-like ground stub," *AEU-Int. J. Electron. Commun.*, Vol. 117, 1–10, 2020.
14. Tang, Z. J., J. Zhan, and X. F. Wu, "Simple ultra-wider-bandwidth MIMO antenna integrated by double decoupling branches and square-ring ground structure," *Microw. Opt. Technol. Lett.*, Vol. 62, No. 3, 1259–1266, 2020.
15. Ali, W. A. E. and A. A. Ibrahim, "A compact double-sided MIMO antenna with an improved isolation for UWB applications," *AEU-Int. J. Electron. Commun.*, Vol. 82, 7–13, 2017.
16. Zhang, S. and G. Pedersen, "Mutual coupling reduction for UWB MIMO antennas with a wideband neutralization line," *IEEE Antennas Wireless Propag. Lett.*, Vol. 15, 166–169, 2016.
17. Wani, Z. and D. Kumar, "A compact  $4 \times 4$  MIMO antenna for UWB applications," *Microw. Opt. Technol. Lett.*, Vol. 58, 1433–1436, 2016.
18. Kumar, A., A. Q. Ansari, B. K. Kanaujia, J. Kishor, and S. Kumar, "An ultra-compact two-port UWB-MIMO antenna with dual band-notched characteristics," *AEU-Int. J. Electron. Commun.*, Vol. 114, 1–12, 2020.
19. Zhao, X., S. P. Yeo, and L. C. Ong, "Planar UWB MIMO antenna with pattern diversity and isolation improvement for mobile platform based on the theory of characteristic modes," *IEEE Trans. on Antennas and Propag.*, Vol. 66, No. 1, 420–425, 2018.
20. Li, H., B. K. Lau, Z. Ying, and S. He, "Decoupling of multiple antennas in terminals with chassis excitation using polarization diversity, angle diversity and current control," *IEEE Trans. Antennas Propag.*, Vol. 60, No. 12, 5947–5957, 2012.